

Experimental study of the variation of the plasma temperature with the laser flux

B K SINHA, N GOPI and S K GOEL

Laser Section, Bhabha Atomic Research Centre, Bombay 400 085

MS received 25 September 1978; revised 6 January 1979

Abstract. Experiments performed with a 50 MW – 60 nsec ruby laser to estimate the temperature of the plasma produced on the planar targets of carbon as well as polyethylene are reported. Temperatures were estimated by two foil ratio technique. The temperatures of carbon and polyethylene plasma show a $\phi^{2/9}$ dependance on flux in the flux regime of 10^{10} W/cm² to 5×10^{11} W/cm². The comparatively slower dependance is explained on the basis of purely collisional absorption, the effect being enhanced due to relatively long duration of the laser pulses. Scaling laws of plasma temperature against laser flux obtained by different workers in different flux regimes have been analysed on the basis of collisional and non-collisional absorption.

Keywords. Plasma heating; plasma diagnostics; plasma production; laser beam heating.

1. Introduction

The two-foil ratio technique, first reported by Jahoda *et al* (1960) has been a very important and relatively reliable tool to determine the plasma temperature for a laser produced plasma. Many experiments (Puell *et al* 1970; Facquignon and Floux 1970; Ahmed and Key 1972; Donaldson *et al* 1973; Yamanaka *et al* 1972, Kang *et al* 1973; Pepin and Grek *et al* 1977 and Galanti and Peacock 1975) have been performed using a high power Nd:glass laser or a CO₂ laser to establish a scaling law of the plasma temperature against flux density in different flux regimes. Most of these use Nd:gl asslaser in the laser pulse-width range of 4-10 nsec. However, very little experimental data are available for a plasma produced by a CO₂ laser, and therefore, it is difficult to comment on the effect of wavelength on the scaling law. The second variable which has a pronounced effect on the hydrodynamics of plasma formation and, hence on the absorptivity of the plasma itself is the pulse width of the laser. Here again, details are lacking as to the effect of this variable but Kang *et al* (1973) did not find any noticeable influence of this parameter when the laser pulse width varied from 4–10 nsec. The third and an important variable is the flux density. Data reported by various workers mentioned earlier are available in different flux regimes varying approximately from 5×10^{11} W/cm² to 7×10^{13} W/cm². The threshold for parametric instability for a glass laser is approximately 10^{12} W/cm² (Nishikawa 1968; Kaw and Dawson 1969; Shearer and Duderstadt 1972; Shearer *et al* 1972; Fabre and Stenz 1974; Krishan *et al* 1976 and Grek *et al* 1977). Based on the available experimental data this regime can be divided into (i) highly anomalous (greater than 2×10^{13} W/cm²), (ii) purely anomalous (5×10^{12} W/cm² to 2×10^{13} W/cm²)

and (iii) collisional and anomalous (5×10^{11} to 5×10^{13} W/cm²). In these three regimes approximate scaling laws are (1) $\phi^{1.2}$, (2) $\phi^{2/3}$ or $\phi^{6/9}$ and (3) $\phi^{4/9}$ or $\phi^{3/9}$. Using a 50 MW – 60 nsec ruby laser we have further extended our work in the purely collisional regime of 10^{10} to 5×10^{11} W/cm² and obtained a scaling law of $\phi^{2/9}$. Since, the pulse width of our laser is also 60 nsec, this changes the hydrodynamics of the problem as the heating is less efficient for high duration pulses (Fader 1968). As the laser absorption in the fourth regime is purely collisional through inverse bremsstrahlung process, scaling law in this regime reflects the efficiency of heating only through this process. In purely anomalous and highly anomalous regimes, the absorption is purely non-collisional through the excitation of parametric instabilities and the scaling law reflects the rate of transfer of energy from the laser beam into the plasma particles via the plasma waves when the waves grow exponentially and saturate. We report in the following experiments performed to study the scaling law in the fourth regime, the model adopted for the calculations and the results obtained.

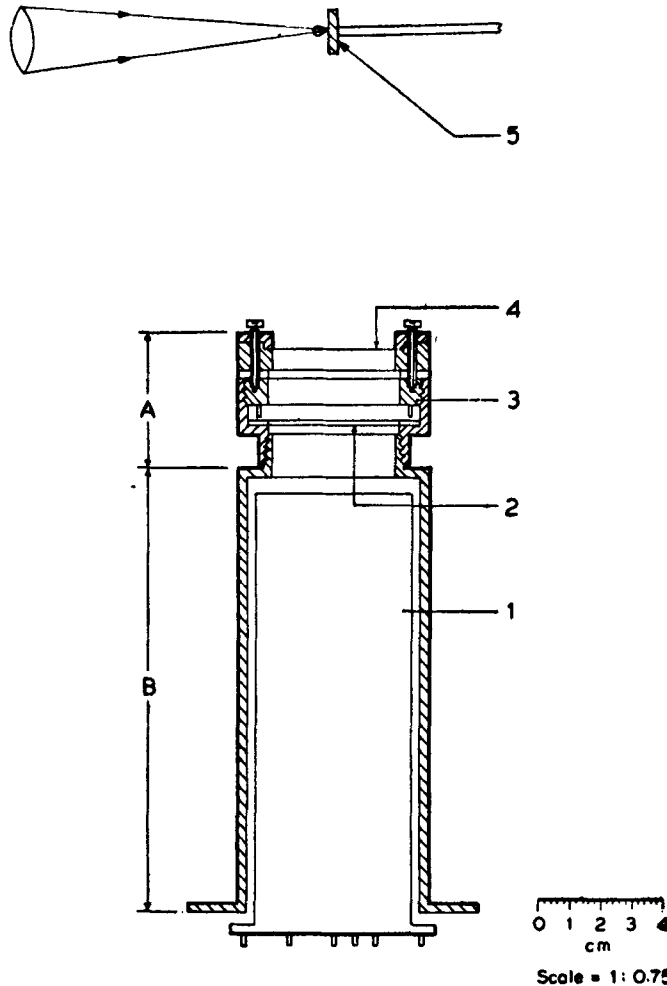


Figure 1. Experimental set up with scintillator detector assembly.

2. Experimental set-up

The experimental set-up is briefly sketched in figure 1. It consists the photomultiplier tube mount (part A) and the scintillator-cum-metallic foil mount (part B) with a provision to obtain the vacuum behind the foil. Parts 1 to 4 represent the RCA 6810 A photomultiplier tube, the 1 mm thick NE 102 plastic scintillator, helical groove to provide vacuum behind the foil, and the foil itself. Since experiments were conducted in low power regime, the x-ray filter used in this experiment was a polycarbonate film, aluminised on both sides. The foil, supplied by Alexander Vacuum Research Company, Massachusetts and code-named B-10, had polycarbonate as base film of thickness 80^{-5} inches and had a total density of 0.25 mg/cm^2 . This density represented 80% thickness of the base film and the remaining represented the thickness of the aluminium. X-ray and laser signals were simultaneously recorded on Tektronix 7633 storage oscilloscope which was triggered by the laser pulse. The x-ray signal through one B-10 foil at a flux density of $2 \times 10^{11} \text{ W/cm}^2$ was high and therefore the ratio of detector noise to x-ray signal was small. At a flux density of $2 \times 10^{11} \text{ W/cm}^2$ the ratio for carbon varied approximately from 0.01 for the signal through one foil to 0.2 for the signal through five foils. The ratio for polyethylene was approximately 0.01 and 0.3 respectively.

The laser consisted of a 50 MW-60 nsec ruby laser operated in a dye Q-switched mode. The polyethylene and carbon targets were planar, 25 mm in diameter and 10 mm in thickness. The laser pulses were focussed with the help of a $f/2$ lens with a focal length of 75 mm. The focal diameter, measured by determining the crater diameter produced by the laser beam and examined on a metallurgical microscope using a Kellner eye piece, was found to be approximately $100 \mu \pm 10 \mu$. The flux density could be varied between $2 \times 10^{10} \text{ W/cm}^2$ and $5 \times 10^{11} \text{ W/cm}^2$. The laser had a pulse duration of 60 nsec and during the course of the experiments the laser pulse was found to be reasonably reliable within 10% of intensity fluctuation.

3. Theoretical calculations

The electron temperatures are estimated by measuring the intensity ratio of soft x-rays transmitted through various absorbers of different thicknesses (Jahoda *et al* 1960; Ahmed and Key 1972; Donaldson *et al* 1973; Kang *et al* 1973). Assuming a Maxwellian distribution of electrons, the intensity I_ν of the bremsstrahlung radiation which has a photon energy of $E=h\nu$ is given by

$$I_\nu = C \frac{n_e n_i Z^2}{(kT_e)^{1/2}} g_{ff} \exp(-h\nu/kT_e), \quad (1)$$

where n_e , n_i are electron and ion densities and Z , T_e are charge number and electron temperature respectively and g_{ff} is the gaunt factor. The intensity I'_ν of the x-ray transmitted through a metal foil of absorption coefficient $\mu(\nu)$ and thickness t_n , where ν is the photon frequency is given by

$$I'_\nu = C \frac{n_e n_i Z^2}{(kT_e)^{1/2}} g_{ff} \exp[-E/kT_e - \mu(\nu)t_n]. \quad (2)$$

Therefore the total intensity I_n of x-rays transmitted through the foil is

$$I_n = \int_0^{\infty} I'_\nu d\nu. \quad (3)$$

The total intensity ratio transmitted through the metal foils of thickness t_1 and t_2 is given by

$$\frac{I_1}{I_2} = \frac{\int_0^{\infty} \exp \{ -hv/kT_e - \mu(\nu) t_1 \} d\nu}{\int_0^{\infty} \exp \{ -hv/kT_e - \mu(\nu) t_2 \} d\nu}. \quad (4)$$

To obtain the various temperatures the left hand side of expression (4) was derived experimentally and that of the right hand side calculated theoretically.

The x-ray flux from the laser plasma consisted of three parts (i) bremsstrahlung emission; (ii) recombination radiations and (iii) line radiations. For high temperature

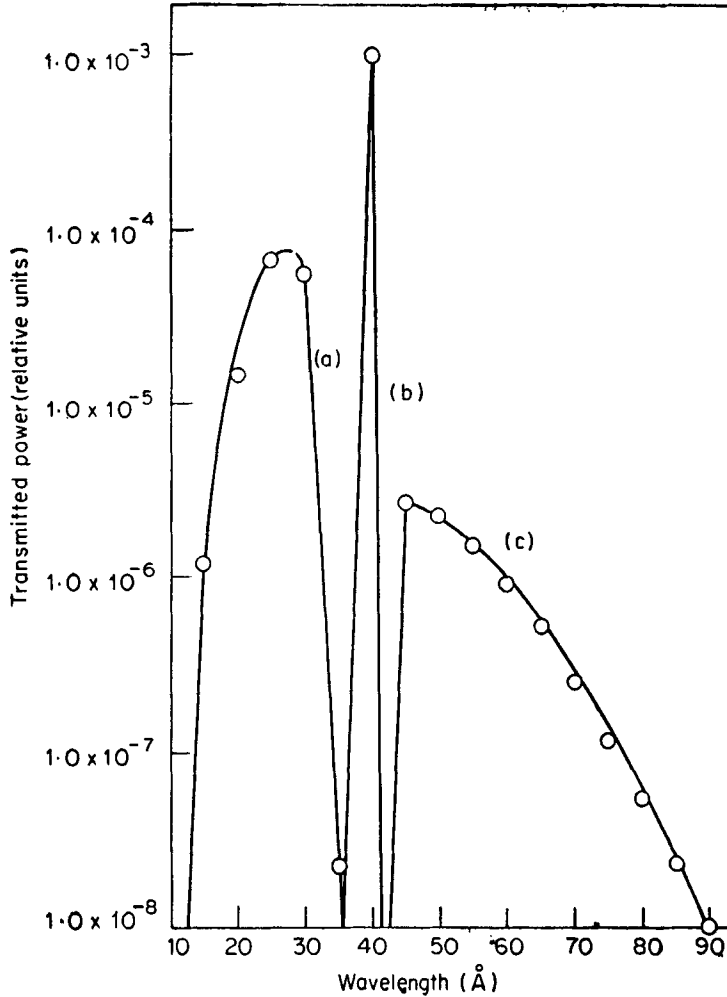


Figure 2a. Spectral profile of transmitted radiation through B-10 foil at 50 eV.

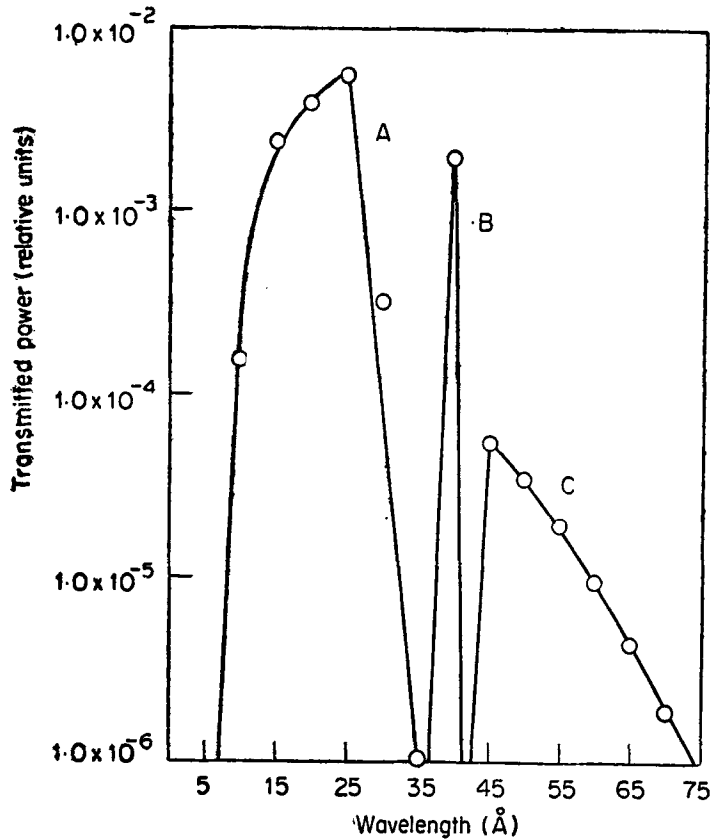


Figure 2b. Spectral profile of transmitted radiation through one B-10 foil at 100 eV.

plasma, the line radiations could be ignored. Since recombination radiation shows the same exponential dependance on temperature as the bremsstrahlung emission, the method described above can be taken as reasonably satisfactory. However, this is not true for low temperature plasma, and this fact is evident from figures (2a) and (2b) in which the zones *A*, *B*, and *C* respectively represent contributions due to recombination, line and bremsstrahlung radiations for a carbon target. At higher temperatures the influence of line radiation decreases. Therefore, using the steady state corona model (Huddleston 1965; Puell 1970; Mallozi *et al* 1972 and Colombant and Tonon 1973; Rager and Robouch 1975), relative magnitudes of bremsstrahlung, recombination and line radiations were calculated. The use of corona model was found necessary as McWhirter's relation (McWhirter 1965) for the validity of the local thermodynamic equilibrium model breaks down. This is seen by applying the approximate rule of thumb given by McWhirter (1965).

$$n_e \leq 10^{16} (T_e)^{7/2} \text{ cm}^{-3}. \quad (5)$$

The quantity T_e is the electron temperature expressed in electron volts. Whenever equation (5) is satisfied, the LTE model breaks down. The absorption coefficient of aluminium was taken from the data of Henke (1967). For the other constituents

of the poly-carbonate base film of the filter, Victoreen's (1949) formula was used. According to the steady state corona model for plasma equilibrium the relative population of charged species is given by

$$\frac{n(z, g)}{n(z+1, g)} = 7.87 \times 10^{-9} [\chi(z, g)]^2 \left[\frac{\chi(z, g)}{kT_e} \right]^{3/4} \exp \left[\frac{\chi(z, g)}{kT_e} \right] \quad (6)$$

where $n(z, g)$ = density of ions in the ground state with charge z .

$n(z+1)g$ = density of ions in ground state with charge $z+1$.

kT_e = the plasma temperature in electron volts.

$\chi(z, g)$ = ionisation potential (in eV) of ions in the ground state with charge $(z+1)$.

From the relative population of different charge states, the following expressions given by Puell (1970) have been used to calculate the relative magnitudes of three types of radiations:

$$P_{ff}(\nu) = 1.7 \times 10^{-47} \cdot (\chi_H/kT_e)^{1/2} n_e \sum_z n_i(z) z^2 \exp(h\nu/kT_e), \quad (7)$$

where $P_{ff}(\nu)$ = bremsstrahlung radiation in W/cm² per unit frequency interval at ν ,

χ_H = hydrogen ion potential in eV,

$h\nu$ = photon energy in eV.

$$P_{fb}(\nu) = 1.7 \times 10^{-47} \cdot \left(\frac{\chi_H}{kT_e} \right)^{3/2} n_e \sum_z n_2(z) \sum_n \left(\frac{\chi_n}{\chi_H} \right)^2 \frac{\tau_n}{n} \exp \left(\frac{\chi_n h\nu}{kT_e} \right) \quad (8)$$

$(h\nu > \chi_n),$

where $P_{fb}(\nu)$ = free bound or recombination radiation in W/cm² per unit frequency interval at ν ,

χ_n = energy required in (eV) to ionise an ion with charge $(z-1)$, by removing an electron in n th shell, where n is the main quantum number,

τ_n = the number of unoccupied sites in n th shell.

$$P_l = 3.5 \times 10^{-25} \cdot \frac{n_e}{(kT_e)^{1/2}} \sum_z n_i(z) \exp \left[-\frac{E(z)}{kT_e} \right] \quad (9)$$

where P_l = line intensity in W/cm²,

$E(z)$ = photon energy in eV for a particular transition and the summation is over all the lines and all the charged particles.

After calculating the relative magnitudes of the three types of radiations, the transmitted intensity I_T through different foils of different thicknesses are obtained by

$$I_T(\nu) = I_l(\nu) \exp \left[-\sum_i K_i(\nu) t_i \right], \quad (10)$$

where $I_l(\nu) = P_{ff}(\nu) + P_{fb}(\nu) + P_l(\nu).$ (11)

$P_{fb}(\nu)$ is included only for $h\nu$ and $P_i(\nu)$ only if there is any line radiation with frequency ν . Here (i) runs over all the foils and $K_i(\nu)$ and t_i are corresponding absorption coefficients and thickness of the i th foil. From the transmitted intensities at different frequencies, the total integrated intensities are calculated by numerically integrating $I_T(\nu)$ over the whole spectrum varying from 1 Å to 100 Å.

4. Theoretical and experimental results

Figures (2a) and (2b) show the spectral profile of the relative transmission through one and two B-10 foils at a temperature of 50 eV. At higher temperatures, the contribution due to line emission decreases in comparison to continuum radiations. Figures (3a) and 3(b) shows the relative transmission of x-ray flux through one and two B-10 foils at a temperature of 100 eV. From the figures, it is clear that the relative magnitude of line emissions at higher temperatures and increasing number of

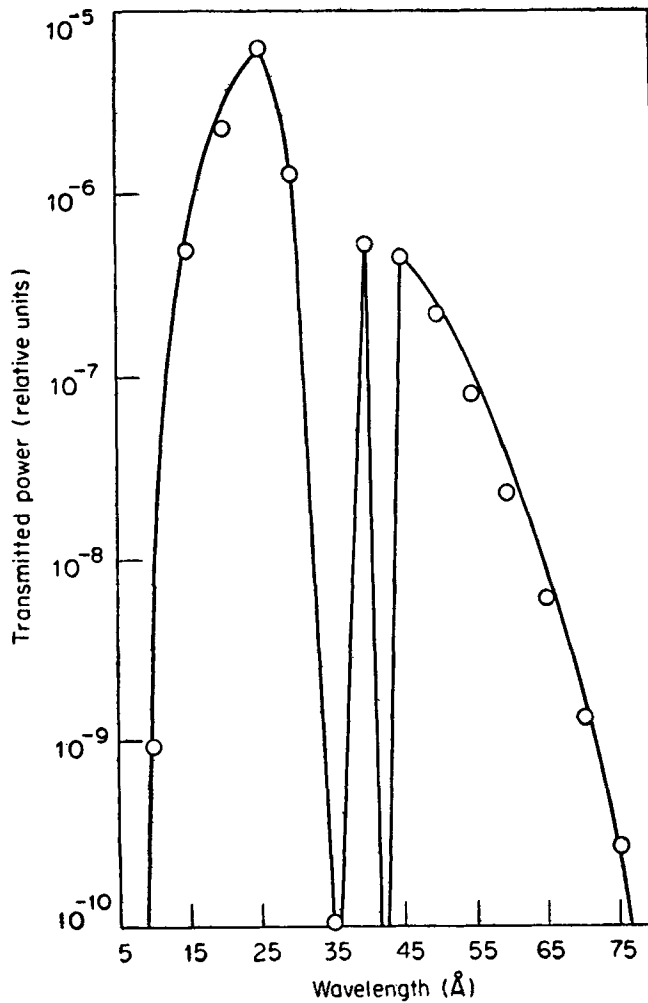


Figure 3a. Spectral profile of transmitted radiation through two B-10 foils at 50 eV

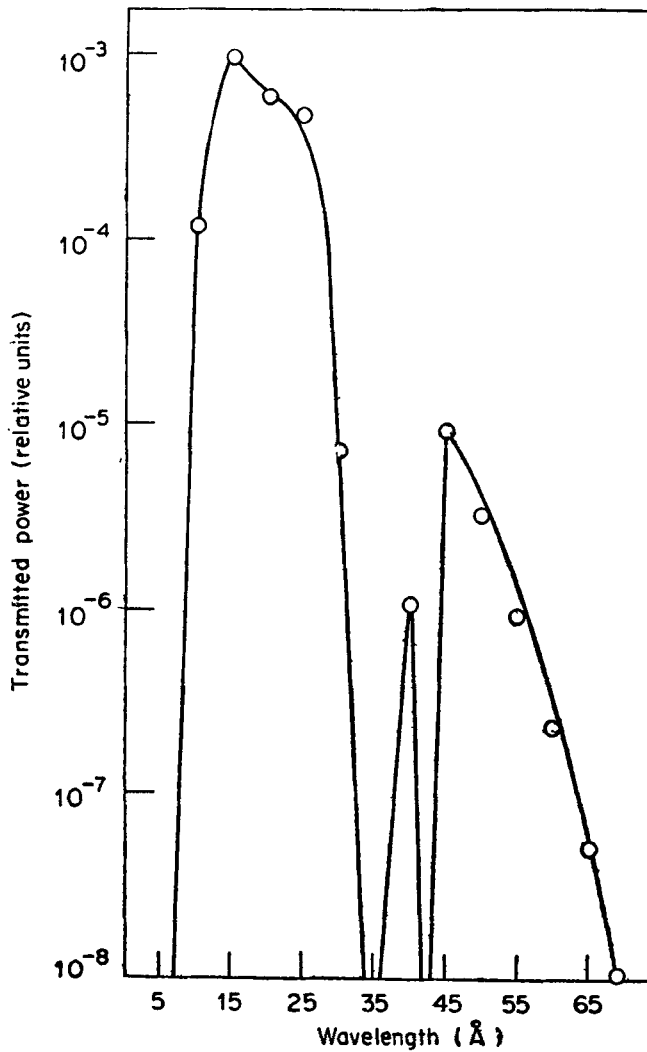


Figure 3b. Spectral profile of transmitted radiation through two B-10 foils at 100 eV.

foils decreases with respect to continuum radiations. Sinha (1979) observed that at temperatures above 50 eV and at increasing number of foils, the most predominant contribution comes from recombination radiation only and the other two radiations, in fact, can be ignored. He found that although the ratio of total radiation-to-recombination radiation at 50 eV through one, two, three, four and five foils is 2.63, 1.21, 1.18, 1.12 and 1.05 respectively the same figure at 100 eV is 1.53, 1.02, 1.00, 1.00 and 1.00 respectively. Ahmed and Key (1972) estimated the plasma temperature with the transmission bands varying between 5 Å and 35 Å and measured the absolute x-ray flux from the plasma assuming the efficiency of 1 photon per keV x-ray energy for the NE 102 scintillator based on the data from Meyrott *et al* (1964). Though our transmission bands vary between 12 Å and 90 Å the main contribution to x-ray flux at temperatures above 50 eV and increasing number of foil-thickness comes only

from within 12 \AA to 35 \AA . Therefore even for absolute x-ray flux measurements the linearity of NE 102 scintillator with respect to energy conversion by soft x-rays can be reasonably assumed.

Figures 4 and 5 are the oscilloscope traces of four x-ray pulses for four laser shots through a B-10 foil from a polyethylene plasma. The left hand side of each pulse train is the laser pulse and the right hand side is the corresponding x-ray pulse. By measuring the laser pulse height as well as the corresponding x-ray pulse height it is seen that the pulses are reasonably reproducible. Secondly, we note that the duration of the x-ray pulse is almost the same as that of the laser pulse.

Figure 6 shows the theoretical and experimental variation of relative x-ray intensity with the foils. Quantities $1t$, $2t$, $3t$, etc stand for one foil thickness, two foil thickness and so on. Theoretical calculations were made between 10 eV to 225 eV and only the relevant theoretical curves are plotted here. Curves A_1 , A_2 , B_1 and B_2 are the theoretical curves at temperatures 135 eV , 125 eV , 75 eV and 65 eV respectively. As the ratio of noise-signal to x-ray flux through four and five B-10 foils for polyethylene started approximating 0.3 , these points were ignored. The plasma temperature for polyethylene then turned out to be 70 eV . The slope of the carbon curve

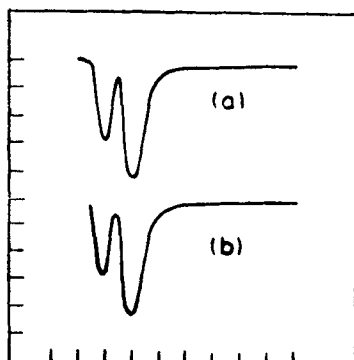


Figure 4. Oscilloscope trace of successive laser and x-ray pulse for a polyethylene plasma.

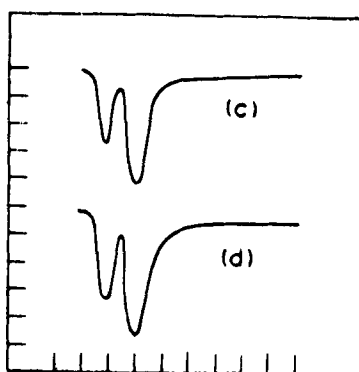


Figure 5. Oscilloscope trace of successive laser and x-ray pulse for a polyethylene plasma.

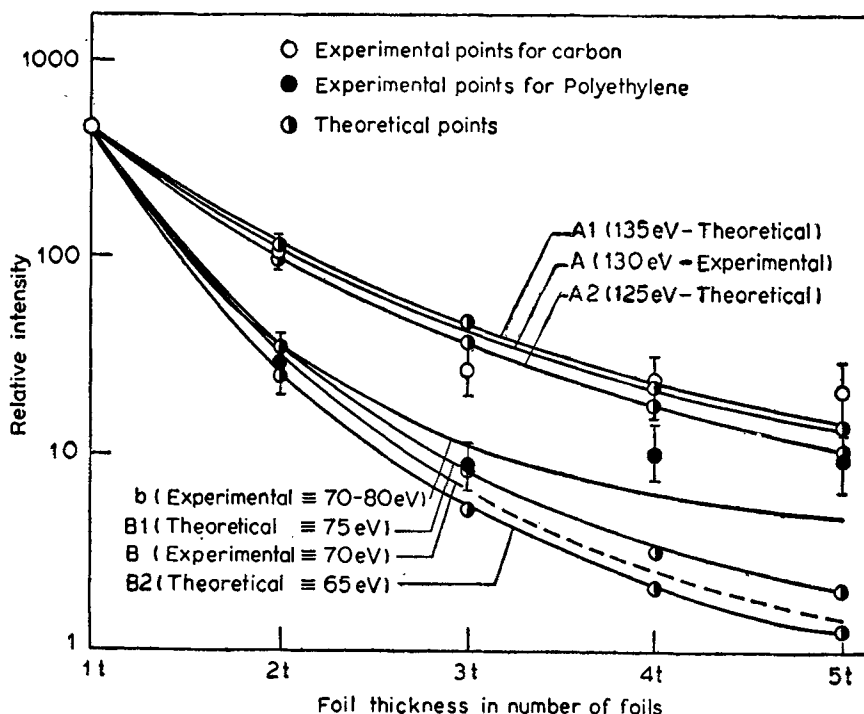


Figure 6. Variation of relative x-ray intensity with number of foils. A for carbon, B for polyethylene.

is reasonably constant pointing to a single temperature plasma which is true for such low temperature experiments. The ratio of x-ray signals due to one foil and two foils and that due to two foils and four foils is found to be approximately 4.5. The same ratio for polyethylene is found to be 10 and 7 respectively. This is true because in the case of polyethylene plasma the measurements of x-ray intensities for four and five foils gave a 30% error. The surface of the polyethylene target was more shining and hence more reflecting than that of carbon. This probably explains the smaller absolute temperature of the former.

Figure 7 represents the variation of relative x-ray intensity with laser flux for carbon and polyethylene. All the x-ray intensities have been measured with respect to the x-ray intensity produced by a laser flux of 2×10^{11} W/cm² through one B-10 foil at the same experimental conditions. Using this experimental observation and coupling with theoretical calculations the variation of plasma temperature with laser flux was obtained. Compared to plasma temperature variation shown in figure 8 the x-ray flux shows a stronger variation on laser flux. The x-ray flux shows approximately a $\phi^{5/9}$ and $\phi^{6/9}$ dependance on laser flux for carbon and polyethylene respectively. Therefore, if there is a fluctuation of 10% in laser flux this will give rise to an error of 5.5% and 6.5% respectively in the x-ray flux, but only 2.2% in the plasma temperature. This is because plasma temperature has $\phi^{2/9}$ dependance on temperature as shown in figure 8. Figure 8 also shows the observed variation of plasma temperature against laser flux. The plasma temperature varies approximately as $\phi^{2/9}$ on laser flux in both the cases.

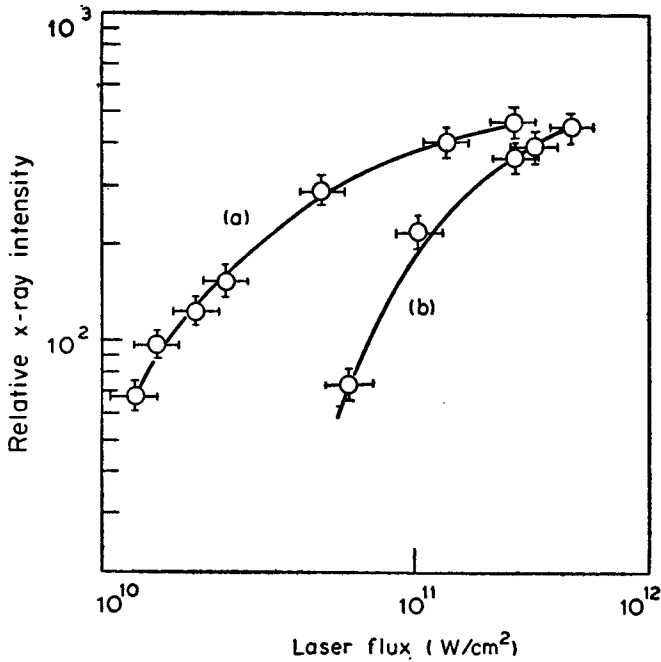


Figure 7. Variation of x-ray intensity with laser flux for carbon (A) and polyethylene (B).

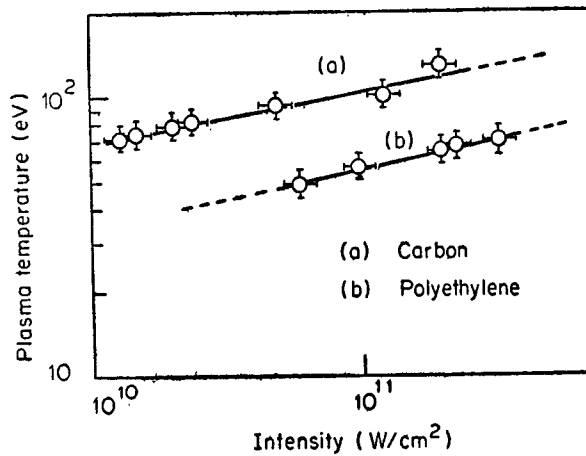


Figure 8. Variation of plasma temperature with flux for carbon (A) and polyethylene (B).

Figure 9 shows the results obtained mostly with Nd:glass laser by various workers in different regimes of flux density. The schematic variation of plasma temperature with flux density in different regions of flux intensity could be seen from the figure. Temperatures plotted closely agree with the experimental results. But due to discontinuities in experimental results obtained by different workers at the beginning

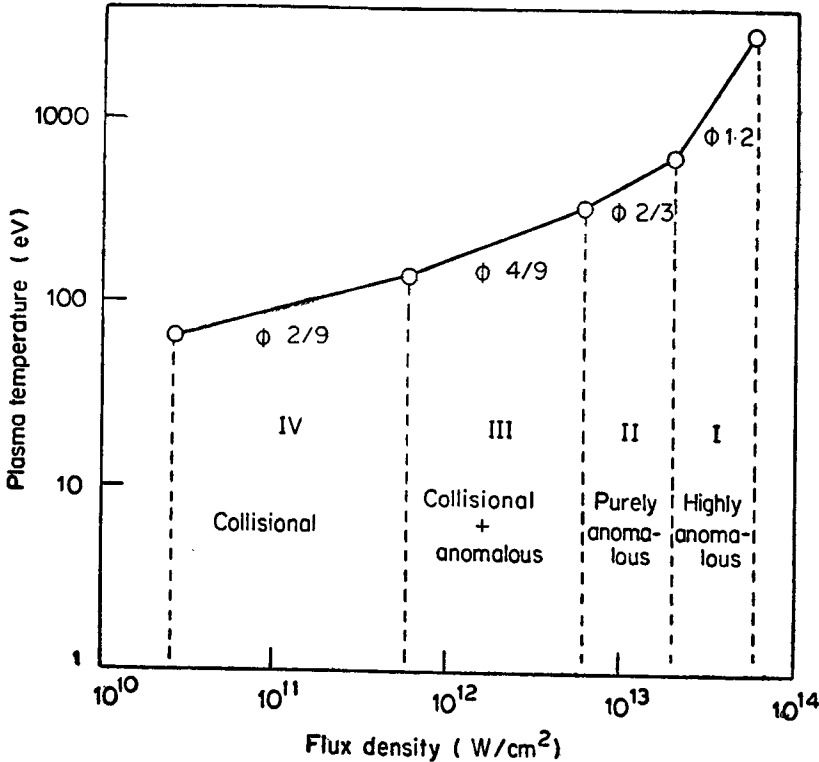


Figure 9. A tentative schematic diagram of the scaling law of plasma temperature against flux.

or end of each regime, some error is likely to be present but the general variation is expected to remain unchanged. The flux regimes have been divided into four zones (1) highly anomalous between 2×10^{13} W/cm² and above; (2) purely anomalous between 6×10^{12} to 2×10^{13} W/cm²; (3) collisional plus anomalous between 6×10^{11} to 6×10^{12} W/cm² and (4) purely collisional between 10^{10} to 6×10^{11} W/cm². The figure shows the dependance of plasma temperature on flux as $\phi^{1.2}$, $\phi^{2/3}$, $\phi^{4/9}$ or $\phi^{3/9}$ and $\phi^{2/9}$ respectively for the four zones.

5. Discussion

Theoretical scaling law of the plasma temperature T_e against laser flux density strongly depends upon the absorption mechanism and the model chosen for expansion hydrodynamics. The mechanism for the absorption further depends upon the laser wavelength (Shearer and Duder-Stadt 1972) and the intensity of laser radiation. Earlier studies of Krokhin (1965), Caruso and Gratton (1968) and Afanasyev *et al* (1969) used an one-dimensional flow approximation and obtained $\phi^{1/2}$ dependance of temperature T_e on the laser flux. The one-dimensional flow is non-stationary in that the temperature increases with time as the plasma flows towards the incoming laser light. The model is unreliable for long duration pulses because it does not consider the radial expansion of the plasma and the consequent decrease in the absorptivity.

Fauquignon and Floux (1970), using a 2-gigawatt, 35 nsec Q-switched neodymium glass laser, performed experiments on solid deuterium target and obtained a $\phi^{2/3}$ dependance of temperature on flux. In their theoretical model, they considered total energy as the sum of the energy of the shocked material and of the plasma (enthalpy, kinetic energy and radiative losses). They completely ignored the energy spent in the kinetic expansion of the plasma and analytically obtained the dependance of plasma temperature. They also experimentally verified their results. Puell (1970) has proposed a model and has partly taken into account the kinetic expansion of the plasma while it is heated and has given a $\phi^{4/9}$ dependance of plasma temperature on flux. Puell *et al* (1970) experimented with 7 nsec pulses on carbon and lithium deuterite and obtained an experimental verification of their model. Lack of experimental data necessary to form a scaling law against wavelength in different intensity regimes makes it difficult to analyse the problem. Though pulse duration of the laser strongly influences the expansion hydrodynamics of the plasma, the role of the pulse-width on the scaling law cannot be convincingly discussed because of inadequate experimental data. Kang *et al* (1973) reported that there was no noticeable influence of pulse width in the scaling law of plasma temperature against flux in the pulse width regime between 4 and 10 nsec. This might be because of the small range of variation of the pulse width. Since our laser pulse has a 60 nsec pulse duration, a significant amount of energy is consumed in the expansion and slower dependance of temperature on flux. Dawson (1964) theoretically studied the temperature produced by a steady state laser on spherical targets and observed that whereas for short periods the expansion is unimportant, for longer periods, (say greater than 20 nsec for a flux of 10^{12} W/cm²), 75% of the laser energy is used up for expansion and 25% for thermal energy of the plasma. Though the role of the pulse width on the scaling law cannot be fully discussed due to inadequate data, we have considered the scaling laws obtained by different workers in different intensity regimes. On this basis we divide the intensity regimes into tentatively four zones as shown in figure 9. In the fourth zone at which the reported experiments are performed, the heating process is mainly controlled by classical absorption through a purely collisional process. The third zone consists of collisional and non-collisional heating (Puell *et al* 1970; Donaldson *et al* 1973; Pepin *et al* 1977; Grek *et al* 1977 and Kang *et al* 1973) where both the absorption processes can be taken as equally dominant since the threshold for parametric instability starts approximately from a flux density of 10^{12} W/cm² for Nd:glass laser. The second zone between 5×10^{12} W/cm² and 2×10^{13} W/cm² can be taken as purely anomalous and the heating is still more efficient Fauquignon and Floux 1970, Yamanaka *et al* 1972). In the first zone (Yamanaka *et al* 1972) the growth rates of the parametric instabilities are known to be very fast and the individual plasma waves tend to saturate and heat the plasma much more efficiently making the anomalous effect more effective. When the available experimental data are compared with our experiments, the scaling laws of plasma temperature against flux density can be taken as (i) $\phi^{1.2}$ in the highly anomalous or turbulent regime (ii) $\phi^{2/3}$ in a purely and mildly anomalous regime (iii) $\phi^{4/9} - \phi^{3/9}$ in collisional plus anomalous regime (Pepin *et al* 1977) and (iv) $\phi^{2/9}$ in a purely collisional regime. However, in order to obtain a clear picture of the scaling laws, and to assess the role of expansion hydrodynamics due to laser pulse width and that of wavelength using a CO₂ laser in all the four intensity regimes, more experiments are necessary.

References

- Afanasyev Y V *et al* 1969 *Sov. Phys. JETP* **10** 353
Ahmed N and Key M H 1972 *J. Phys.* **B5** 866
Caruso A and Gratton R 1968 *Plasma Phys.* **10** 867
Colombant D and Tonon G 1973 *J. Appl. Phys.* **44** 3524
Dawson J M 1964 *Phys. Fluids* **7** 981
Donaldson T P *et al* 1973 *J. Phys.* **B6** 1525
Fabre E and Stenz C 1974 *Phys. Rev. Lett.* **32** 823
Fader W J 1968 *Phys. Fluids* **11** 2200
Fauquignon C and Floux F 1970 *Phys. Fluids* **13** 386
Galanti M and Peacock N J 1975 *J. Phys.* **B8** 2427
Grek B *et al* 1977 *Nucl. Fusion* **17** 1165
Henke B 1967 *Noretco Rep.* **14** 112
Huddleston R 1965 *Plasma diagnostic technique* (New York : Academic Press)
Jahoda F C *et al* 1960 *Phys. Rev.* **119** 843
Kang H B *et al* 1973 *J. Phys. Soc. Jpn.* **34** 504
Kaw P K and Dawson J M 1969 *Phys. Fluids* **12** 2586
Krishan V *et al* 1976 *Appl. Phys. Lett.* **29** 90
Krokhin U N and Gratton R 1969 *Plasma Phys.* **10** 867
Mallozi P *et al* 1972 *Report on x-ray emission from laser generated plasma, Battelle Columbus Lab.*
Meyrott A J *et al* 1964 *Rev. Sci. Instrum.* **35** 669
McWhirter R W P 1965 in *Plasma diagnostic techniques* eds R H Huddleston and S L Leonard,
Ch. 5 (New York: Academic Press)
Nishikawa K 1968 *J. Phys. Soc. Jpn.* **24** 916
Pepin H and Grek 1977 *J. Appl. Phys.* **48** 3312
Puell H 1970 *Z. Naturforschung* **A25** 1807
Puell H *et al* 1970 *Z. Naturforschung* **A25** 1815
Rager J and Robouch B 1975 *Appl. Phys. Lett.* **26** 664
Shearer J *et al* 1972 *Phys. Rev.* **A6** 764
Shearer J and Duderstadt J 1972 *Univ. of California, Lawrence Livermore Lab. Rep. No. UCRL-74094*
Sinha B K 1979 *Appl. Phys. Lett.* (submitted)
Victoreen J 1949 *J. Appl. Phys.* **20** 1141
Yamanaka C *et al* 1972 *Phys. Rev.* **A6** 2335